



wire through the anode spot being uniformly distributed over its section $z = L_w$. In addition, the entire wire is heated by arc current I flowing through it. It is assumed that the wire is in transverse position relative to the plasma flow around it at distance Z_w from the exit section of the plasma torch nozzle, and that the exit section of the wire feeder nozzle is at distance L_p from the plasma torch axis. Also, it is assumed that the wire melting rate is equal to the wire feed speed, and that the molten metal crossing section $z = L_w$ is detached and carried away by the plasma flow.

The thermal state of the anode wire under the plasma arc spraying conditions is determined by a set of the following physical processes: convective-conductive heat exchange of the plasma flow and surrounding gas with the side surface of the wire, thermal radiation energy exchange between the plasma and wire surface, effect of the electric arc introducing heat through the anode spot, volumetric Joule heating of the wire by the electric current flow, losses of heat with the molten metal carried away by the plasma flow, and cooling of the wire surface due to entrainment of the energy of evaporation of its material atoms by the vapour flow.

Assuming that the temperature field in the wire is characterised by the axial symmetry, the problem of finding it is reduced to solving the quasi-stationary thermal conductivity equation written down in the cylindrical coordinate system:

$$\begin{aligned} \gamma_w C_w v_w \frac{\partial T_w}{\partial z} = \frac{1}{r} \frac{\partial}{\partial r} \left(\chi_w r \frac{\partial T_w}{\partial r} \right) + \\ + \frac{\partial}{\partial z} \left(\chi_w \frac{\partial T_w}{\partial z} \right) + j^2 \rho_w, \end{aligned} \quad (1)$$

where $T_w(r, z)$ is the spatial distribution of temperature in the wire; $\gamma_w(T)$, $C_w(T)$, $\chi_w(T)$ and $\rho_w(T)$ are the density, effective specific heat, thermal conductivity coefficient and specific electrical resistance of the wire material, respectively; and j is the density of the electric current.

Consider the statement of boundary conditions for equation (1). Allowing for the above heat exchange mechanisms, the boundary condition on the wire surface (at $r = R_w$) can be expressed as follows:

$$\left(-\chi_w \frac{\partial T_w}{\partial r} \right) \Big|_{r=R_w} = Q_c + Q_r - Q_v, \quad (2)$$

where Q_c is the flow density of the energy due to convective-conductive heat exchange of the wire with the plasma and ambient gas; Q_r is the flow density of the energy of thermal radiation of the plasma absorbed by the wire surface; and Q_v is the flow density of the evaporation energy carried away from the wire surface.

The following symmetry conditions were specified for the wire axis:

$$\frac{\partial T_w}{\partial r} = 0. \quad (3)$$

Assuming that the wire goes out from the nozzle with temperature T_0 , the boundary condition at $z = 0$ will be written down as follows:

$$T_w(r, 0) = T_0. \quad (4)$$

To determine the boundary condition at the molten tip of the wire, it is necessary to allow for the heat released in a region of the anode fixation of the arc, as well as for the heat losses related to evaporation of the wire material and detachment of the melt by the plasma jet. As a result, the boundary condition at $z = L_w$ will be defined as

$$\left(-\chi_w \frac{\partial T_w}{\partial z} \right) \Big|_{z=L_w} = Q_a - Q_v - Q_t, \quad (5)$$

where Q_a is the specific heat flow from the arc to the anode, and Q_t are the heat losses related to detachment and carrying away of the molten material of the wire.

Consider the above components of heat exchange in more detail. The calculation region of the wire is located both in a zone affected by the high-temperature core of the plasma flow heating the wire and in a relatively cold peripheral regions of the flow through which the heat is removed from the wire. Assuming that the spatial distributions of temperature $T_p = T_p(z)$ and velocity $u_p = u_p(z)$ of the plasma along the wire length are known (e.g. calculated on the basis of model [6]), the convective-conductive heat flow under the given conditions can be determined according to the Newton model of heat exchange [7]:

$$Q_c = \alpha(T_p - T_{ws}), \quad (6)$$

where α is the heat transfer coefficient, and $T_{ws}(z) = T_w(R_w, z)$ is the temperature of the wire surface.

Heat transfer coefficient α is related to Nusselt number Nu that characterises the convective heat exchange as follows:

$$\alpha = Nu \chi_p / (2R_w), \quad (7)$$

where $\chi_p(T)$ is the coefficient of thermal conductivity of the plasma.

The Nusselt number in the transverse flow of the argon plasma around a cylinder is determined by the following expression, according to [8]:

$$\begin{aligned} Nu = 0.5 Re^{0.5} Pr^{0.4} (\gamma_p \eta_p / \gamma_{pw} \eta_{pw})^{0.2}, \\ Re = \frac{2R_w \gamma_p u_p}{\eta_p}, \quad Pr = \frac{C_p \eta_p}{\chi_p}, \end{aligned} \quad (8)$$

where Re and Pr are the Reynolds and Prandtl numbers, respectively; $\gamma_p(T)$, $\eta_p(T)$ and $C_p(T)$ are the density, dynamic viscosity and specific heat of the plasma at a constant pressure calculated at a temperature of the undisturbed flow; and $\gamma_{pw} = \gamma_p(T_{ws})$ and



$\eta_{pw} = \eta_p(T_{ws})$ are the density and viscosity of the plasma at a temperature of the wire surface.

The density of the heat flow due to radiation heat exchange can be calculated by using the known relationship [7]:

$$Q_r = \beta \sigma_0 (T_p^4 - T_{ws}^4), \tag{9}$$

where β is the emissivity factor of the wire material, and σ_0 is the Stefan–Boltzmann constant.

The heat flow due to evaporation of the material from the wire surface can be calculated from the following expression:

$$Q_v = \varepsilon nu, \tag{10}$$

where ε is the latent evaporation heat per atom, and n and u are the concentration and velocity of atoms of the metal vapour near the evaporation surface calculated by the procedure from study [9].

Specific heat flow to the anode, Q_a , is determined by a number of technological parameters, such as the arc current, composition of the electrode wire, kind of the plasma gas etc., and is of an order of $(0.8–1.5) \cdot 10^9 \text{ W/m}^2$ under the conditions considered [10].

Heat losses Q_t can be determined proceeding from an assumption that the velocity of the melting front and, hence, detachment of the molten material of the wire is equal to wire material feed speed v_w . Then

$$Q_t = C_w \gamma_w v_w T_w(r, L). \tag{11}$$

As a result, the spatial distribution of temperature in the consumable anode wire during plasma arc spraying can be determined by solving equation (1) with boundary conditions (2)–(5) and closing relationships (6)–(11).

Mathematical formulation of the stated problem can also be presented in a simpler form. For example, although the temperature in a cross section of the wire is distributed non-uniformly, this difference is insignificant. This is related to high thermal conductivity of the material of the spraying wire, as well as to its rather small diameter (about 1–2 mm). Then, integrating equation (1) with respect to radius yields the following unidimensional thermal conductivity equation:

$$\gamma_w C_w v_w \frac{\partial \bar{T}_w}{\partial z} = \frac{\partial}{\partial z} \left(\chi_w \frac{\partial \bar{T}_w}{\partial z} \right) + W, \tag{12}$$

where $\bar{T}_w(z)$ is the wire temperature averaged across the section, and W is the power of the heat sources.

The left and right boundary conditions for equation (12) will preserve the form of (4) and (5), the difference being that temperature $\bar{T}_w(z)$ averaged across the wire section appears in the said relationships instead of wire temperature $T_w(r, z)$. The heat flows through the side surface of the wire that appear in condition (2) transform to the volume heat sources

after integration of equation (1). The power of these sources can be determined from the following formula:

$$W = [I^2 \rho_w / (\pi R_w^2) + 2\pi R_w (Q_c + Q_r - Q_v)] / \pi R_w^2. \tag{13}$$

At this point we can consider description of the model of heating and melting of the wire in plasma arc wire spraying to be completed.

Now consider the procedure for solving the stated problem. Because the coefficients of equation (12), boundary condition (5) and closing relationships (6)–(11) are non-linear, it is very difficult to obtain an analytical solution of this equation. Therefore, the problem considered was solved numerically by the finite difference method [11, 12]. Equation (12) was approximated by the three-point scheme. Non-symmetrical differences against the wire speed were used for approximation of the convective term. The under-relaxation method was employed to improve convergence of the solution [12]. No explicit separation of interface between the phases in the wire was used in the calculations. Instead, the use was made of the shock-capturing method [11]. In this connection, effective heat capacity $\bar{C}_w(T)$ allowing for the latent melting heat was used instead of specific heat $C_w(T)$ of the wire material:

$$\bar{C}_w(T) = C_w(T) + W_w^m \delta(T - T_w^m), \tag{14}$$

where T_w^m is the melting temperature; W_w^m is the latent melting heat of the wire material, and $\delta(x)$ is the delta function.

To evaluate the thermal state of the wire in spraying it is necessary to know distributions of thermal and gas-dynamic characteristics of the flow of the arc plasma in a wire location region. These characteristics were calculated by using the earlier developed software [6] intended for quantitative evaluation of parameters of the turbulent flow of the arc plasma under the plasma arc spraying conditions. It was assumed for the calculations that the anode wire is located at distance $Z_w = 6.3 \text{ mm}$ from the exit section of the plasma torch nozzle. Distributions of the thermal and gas-dynamic characteristics of the plasma in this section under different operating conditions of the plasma torch are shown in Figure 2.

Numerical investigations were carried out for a steel wire, the thermal-physical characteristics of which were taken from study [4]. Wire parameters and spraying conditions were varied within the following ranges: wire diameter 1.4–1.6 mm, wire feed speed 6–15 m/min, arc current 160–240 A, and plasma gas (argon) flow rate 1.0–1.5 m³/h. Distance from the wire tip to the plasma jet axis was varied from 0 to 1 mm, and extension (distance from the feeder nozzle to the wire molten tip) was assumed to be equal to 12 mm.

Consider the modelling results. A very important aspect in analysis of the thermal state of the wire

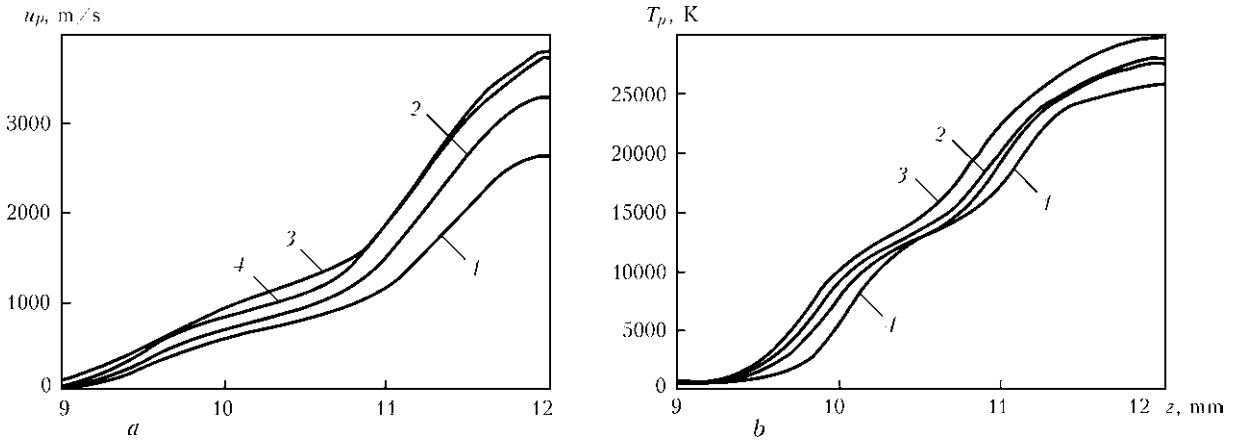


Figure 2. Distribution of velocity (a) and temperature (b) of plasma along the spraying anode wire (molten tip of the wire is located on the plasma jet axis): 1 – $I = 160$; 2, 4 – 200; 3 – 240 A, argon flow rate of $1 \text{ m}^3/\text{h}$; 4 – argon flow rate of $1.5 \text{ m}^3/\text{h}$

during spraying is evaluation of different components of its heat exchange with the arc plasma. Within the problem under consideration, interaction of the wire with external heat sources takes place through its side surface and through the melt on its tip.

Heating of the side surface of the wire is provided by two components – convective and radiation heat exchange with the plasma jet flowing around the wire (Figure 3). Contribution of these components to the energy balance of the spraying wire surface is approximately identical, near the molten tip of the wire the intensity of the said heat sources substantially growing, which is related to high values of temperature (up to 30,000 K) and velocity (up to 3800 m/s) of the plasma in the near-axis zone of the jet. As a result, the temperature of the wire in the $11 < z < 11.9 \text{ mm}$ region may exceed the boiling temperature of its material (3133 K). In this case the wire material intensively evaporates, and the wire cools down (see Figure 3, curve 4). In turn, this leads to a drop of the total heat flow through the side surface of the wire (Figure 3, curve 1). A reversed situation takes place in the wire regions located at a distance from the jet axis, i.e. the wire temperature becomes insignificant, as the wire is cooled by a cold gas flowing around it.

The heat balance of the wire surface region near section $z = L_w$ (see Figure 3) and directly in this section (Figure 4) should be considered separately. It can be seen from Figure 3 that in this region ($11.7 < z < 12 \text{ mm}$) the role of evaporation cooling substantially decreases and, hence, the resultant flow to the wire grows. Because of the direct dependence of values of the heat losses related to evaporation of the wire material on the temperature, this situation is caused by a dramatic decrease in temperature of the wire surface in the given region (Figures 5–8), this being associated with intensive removal of heat through section $z = L_w$. Moreover, the heat losses increase here with increase in temperature (see Figure 4). At low values of the temperature in the given section the heat losses are caused mainly by detachment of the molten material of the wire by the transverse plasma flow. At higher temperatures the key role in the heat balance of the section considered is played by evaporation cooling.

The effect of another heat source, i.e. the energy released due to the electric current flowing through the wire, is of low significance. In particular, contribution of the Joule heating near the molten tip of the wire is less than 1 % of the total action of all the sources (13) heating the wire. Therefore, heating and melting of the wire in plasma arc spraying are provided

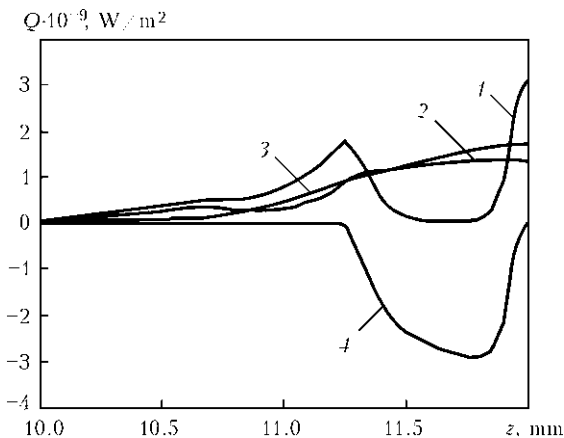


Figure 3. Distribution of components of heat flow along the length of the wire towards its surface ($I = 200 \text{ A}$; argon flow rate of $1 \text{ m}^3/\text{h}$; $2R_w = 1.4 \text{ mm}$; $v_w = 9 \text{ m/s}$, molten tip of the wire is located on the plasma jet axis): 1 – total heat flow; 2 – Q_c ; 3 – Q_r ; 4 – Q_e .

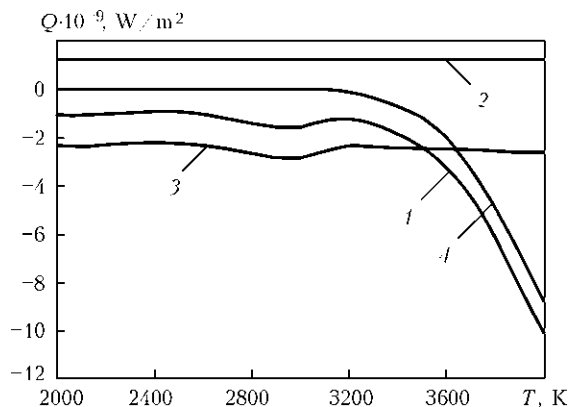


Figure 4. Total heat flow (1) introduced through section $z = L_w$ and its components (2 – Q_a ; 3 – Q_i ; 4 – Q_e) depending on the melt temperature in the given section

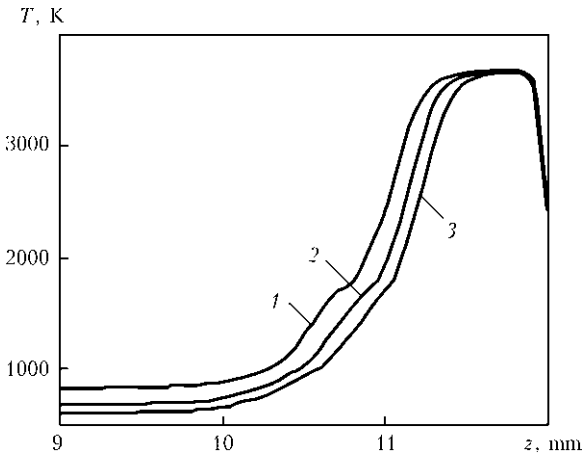


Figure 5. Distribution of temperature along the length of the wire depending on its diameter: 1 – 1.2; 2 – 1.4; 3 – 1.6 mm

primarily by the effect of the high-temperature high-velocity plasma jet.

Figures 5–8 show temperature fields in the wire resulting from variations of technological parameters of the spraying process. The effect of the wire diameter on the limiting-state temperature field is shown in Figure 5. As follows from the calculated data shown in this Figure, in case of heating of the large-diameter wire the length of the region heated above a specified temperature decreases. The same situation takes place also with increase in the wire feed speed. Decrease in the length of the high-temperature region near the molten tip of the wire (Figure 6) in this case results from the fact that the speed of the wire fed to the arc is in excess of the rate of distribution of heat in the wire due to the heat conduction mechanism. In addition, the heat losses due to the molten metal drops grow with increase of the wire feed speed. As a result, at a wire feed speed of 15 m/min the size of the molten region is 0.8 mm, and at a wire feed speed of 5 m/min it amounts to 1.35 mm.

The above results were obtained at an assumption that the molten tip of the wire is located on the plasma jet axis ($L_w = L_p$). Consider now how displacement of the wire tip with respect to the plasma jet axis affects the thermal state of the wire. As follows from

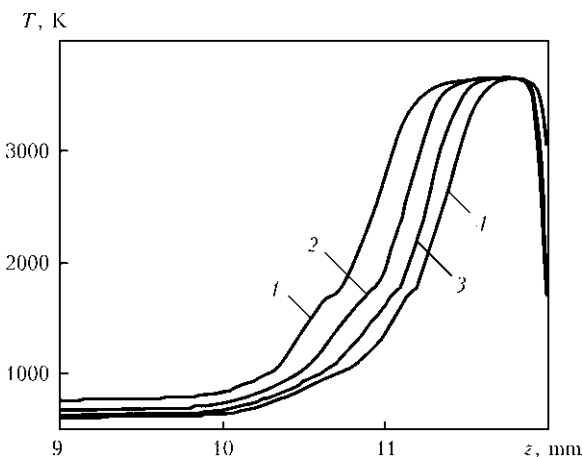


Figure 6. Distribution of temperature in the wire at different wire feed speeds: 1 – 5; 2 – 9; 3 – 12; 4 – 15 m/min

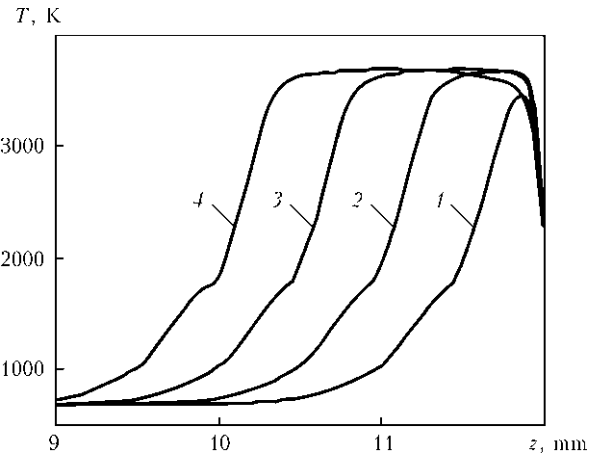


Figure 7. Distribution of temperature along the length of the wire depending on displacement of its molten tip relative to the plasma jet axis: 1 – $L_w - L_p = -0.5$; 2 – 0; 3 – 0.5; 4 – 1 mm

Figure 7, position of the molten tip of the wire has a considerable effect on the size of the heating and melting regions. For instance, if the wire is fed ahead of the plasma jet axis, the area of the side surface affected by the jet core grows. Given that heating of the wire is provided primarily due to the effect of the convective-conductive and radiation heat exchanges, the amount of heat accumulated in the wire increases. As a result, e.g. at $L_w - L_p = 0.5$ mm (see Figure 7, curve 3), the length of the molten region is 1.55 mm. In a case where the molten tip of the wire does not reach the jet axis, thus being on the periphery of the plasma flow, the share of the convective-conductive and radiation heating of the wire substantially decreases. E.g. at $L_w - L_p = -0.5$ mm the length of the molten region is 0.55 mm (Figure 7, curve 1). The results obtained are indicative of the fact that the plasma arc spraying process considered is characterised by the self-regulating possibilities. That is, the certain position of the molten tip of the wire relative to the plasma torch axis and length of the melt held on its tip set in with the spraying process parameters maintained at a steady-state level. Probable fluctuations of the process parameters during spraying lead to a

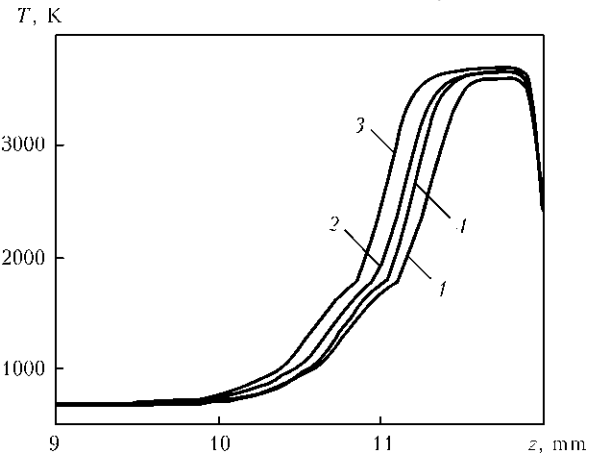


Figure 8. Distribution of temperature along the length of the wire at different operating parameters of the plasma torch: 1 – $I = 160$; 2, 4 – 200; 3 – 240 A, argon flow rate of $1 \text{ m}^3/\text{h}$; 4 – argon flow rate of $1.5 \text{ m}^3/\text{h}$



corresponding change in the above characteristics. However, in this case the amount of the heat input will be either insufficient for heating and melting of the wire and, as a result, it will come to its optimal position, or, if the wire goes ahead of the jet axis, the intensity of heating will be substantially increased and size of the molten metal region will grow as long as it can stay on the wire tip. Detachment of the melt by the plasma jet decreases the length of the wire. As a result, its tip will also come to the optimal position with respect to the jet axis.

Finally, Figure 8 shows the effect of operating parameters of the plasma torch on heating and melting of the spraying wire. At high values of the arc current the plasma velocity and temperature are higher. Hence, the role of the convective-conductive and radiation heat exchanges in the energy balance of the wire and length of its molten tip grow. Increase of the gas flow rate leads, first of all, to increase in the plasma velocity. In this case, the length of the molten region decreases to some extent.

CONCLUSIONS

1. The developed mathematical model can be applied to predict the temperature field and volume of molten metal of the live wire in plasma arc spraying.
2. As established by mathematical modelling, heating and melting of the anode wire in plasma arc spraying are caused primarily by the effect of the high-temperature plasma flow around the wire.
3. The model suggested allowed deriving dependencies of spatial distribution of temperature and volume of molten metal of the wire on such spraying

process parameters as the arc current, plasma gas flow rate and wire feed speed.

4. To construct the complete self-consistent model of the plasma arc spraying process it is necessary to develop a model of flow of the melt at the wire tip and formation of drops of the electrode metal, which, together with the plasma flow and wire heating models, would allow predicting the size, initial temperature and speed of introduction of fine particles formed as a result of melting of the wire to the plasma jet.

1. Kudinov, V.V., Bobrov, G.V. (1992) *Spraying deposition of coatings. Theory, technology and equipment*. Moscow: Metallurgiya.
2. Rykalin, N.N. (1951) *Calculations of thermal processes in welding*. Moscow: Mashgiz.
3. Sanyal, S., Chandra, S., Kumar, S. et al. (2004) An improved model of cored wire injection in steel melts. *ISIJ Int.*, **44**(7), 1157–1166.
4. Hu, J., Tsai, H.L. (2007) Heat and mass transfer in gas metal arc welding. Pt 1: The arc. *Int. J. Heat and Mass Transfer*, **50**, 833–846.
5. Hu, J., Tsai, H.L. (2007) Heat and mass transfer in gas metal arc welding. Pt 2: The metal. *Ibid.*, **50**, 808–820.
6. Kharlamov, M.Yu., Krivtsun, I.V., Korzhik, V.N. et al. (2007) Mathematical model of arc plasma generated by plasmatron with anode wire. *The Paton Welding J.*, **12**, 9–14.
7. Yudaev, B.N. (1988) *Technical thermodynamics. Heat transfer: Manual for non-energy production higher techn. institutions*. Moscow: Vysshaya Shkola.
8. Dresvin, S.V., Donskoj, A.V., Goldfarb, V.M. et al. (1972) *Physics and engineering of low-temperature plasma*. Ed. by S.V. Dresvin. Moscow: Atomizdat.
9. Knight, Ch.J. (1979) Theoretical modeling of rapid surface vaporization with back pressure. *AIAA J.*, **17**(5), 519–523.
10. Nemchinsky, V.A. (1994) Plasma parameters near a small anode in a high-pressure arc (gas metal arc welding). *J. Phys. D: Appl. Phys.*, **27**, 2515–2521.
11. Samarsky, A.A., Vabishchevich, P.N. (2003) *Computational heat transfer*. Moscow: Editorial URSS.
12. Anderson, D., Tannehill, J., Pletcher, P. (1990) *Computational hydromechanics and heat exchange*. Vol. 1. Moscow: Mir.

TO THE ATTENTION OF THE READERS!

The next regular information-statistical book SVESTA-2010: Welding. Robots. Steel (Economical-Statistical Data on Welding Production) is placed on the site of the E.O. Paton Electric Welding Institute of the NAS of Ukraine – www.paton.kiev.ua.

The authors-compilers of the book: [V.N. Bernadsky], O.K. Makovetskaya. Ed. by Prof. K.A. Yushchenko, Prof. L.M. Lobanov. – English language; 119 p.; 94 tables; 90 figures.

Book SVESTA-2010 was prepared and published by the E.O. Paton Electric Welding Institute (PWI) of the National Academy of Sciences of Ukraine with the assistance rendered by the International Institute of Welding (IIW) and European Welding Federation (EWF).

The book contains systematised economic-statistical information on state-of-the-arc and trends in development, consumption and market of welding engineering, as well as on world and national markets of technological welding robots and steel, which was the key structural material in 2006–2009.

The book includes statistical information on the world as a whole and on separate countries – members of IIW of the European, American and Asian regions, such as Bulgaria, Germany, Italy, Poland, Rumania, Great Britain, Russia, Ukraine, Brazil, USA, China, India, Japan, and South Korea. All the information is presented in the form of tables and diagrams, the sources of receiving this information being indicated.

